Available online at www.sciencedirect.com
SCIENCE DIRECT®
Catalysis Today 98 (2004) 123–129
CATALYSIS TODAY
www.elsevier.com/locate/cattod

Synthesis, characterization and comparison of catalytic properties of NiMo- and NiW/Ti-MCM-41 catalysts for HDS of thiophene and HVGO

R. Silva-Rodrigo[a,*], C. Calderón-Salas[a], J.A. Melo-Banda[a], J.M. Domínguez[b], A. Vázquez-Rodríguez[b]

[a]*División de Estudios de Posgrado e Investigación, Instituto Tecnológico de Cd. Madero, Juventino Rosas y Jesús Urueta S/N, Col. Los Mangos, 89440 Cd. Madero, Tam., México*
[b]*Molecular Engineering Program, Instituto Mexicano del Petróleo, 152 Eje Central L. Cárdenas, 07730 México, D.F., México*

Available online 11 September 2004

Abstract

Hydrotreating of heavy oil fractions is usually carried out in fixed bed reactors using alumina-supported Ni-Mo and Co-Mo catalysts. The catalytic properties of hybrid Al- and Ti-MCM-41 materials were compared for HDS of thiophene and heavy vacuum gas oil (HVGO) derived from Maya crude. Upon addition of 20 wt.% TiO_2, the hexagonal symmetry of the pore arrays was unchanged, but the surface area increased from about 1040 up to 1138 m^2/g. In parallel, NH_3-thermal programmed desorption (TPD) studies showed an increase of surface acidity with TiO_2 content, i.e., from 38 μmol NH_3/g for initial MCM-41 to about 62 μmol NH_3/g for 80% Ti-substituted Si-MCM-41. Also, Ni-Mo and Ni-W metal loadings increased the total surface acidity, from about 44 μmol NH_3/g for NiMo/MCM-41 to about 148 μmol NH_3/g for NiMo/MCM-41. Also, the hydrothermal stability of the Ti-MCM-41 materials increased from about 500 °C up to 600 °C under 100% water vapor. Finally, sulfided forms of Ti-MCM-41-supported Ni-Mo and Ni-W catalysts were tested for HDS of heavy vacuum gas oil and thiophene at 350 °C, the NiMo/Ti-MCM-41 and NiW/Ti-MCM-41 catalysts with 50% Ti showing the highest activity, which was comparable to reference catalysts.

Keywords: HDS of HVGO; Deep HDS on Ti-MCM-41; Mesoporous HDT catalysts

1. Introduction

The new environmental regulations on cleaner fuels imply a drastic diminution of sulfur and aromatics with respect to current values, which will contribute further to the abatement of noxious emissions of SO_x, NO_x, CO and refractory polyaromatic compounds. In this respect, deep hydrotreating (DHDT) of heavy oil fractions in refinery processes is of major importance. In many cases, rather than making additional investments for modifying the actual design of HDS refinery plants, HDS/HDN/HDM catalysts are being used under more severe conditions. Those catalysts must withstand higher temperatures, reducing conditions and corrosive atmospheres (H_2S) and metals (V, Ni). In addition, the molecular complexity associated with heavier oil fractions emphasizes the problems related with higher sulfur and metals content. Therefore, a valuable route for improving the catalysts performance implies the search of new large pore materials for HDT catalysts supports, but these materials may possess both structural and textural stability under the conditions mentioned above. Altogether, potential refractory properties of the active phases and higher support stability might result in more useful catalysts for deep HDS and HDN [1–4]. In this viewpoint, large pore materials belonging to the M41S family, which have wide open pores of about 4 nm diameter, might be suitable for enhancing the adsorption and diffusion of complex molecules, provided their structural stability is appropriate to withstand the severe use conditions. Thus, the partial substitution of structural Si^{4+} by polyvalent ions like Ln^{3+}, or grafting Ti^{4+}, Al^{3+}, Fe^{3+} might promote additional stability of the silica pore walls of MCM-41

* Corresponding author. Tel.: +52 833 2158544; fax: +52 833 2158544.
E-mail address: rebsilva@hotmail.com (R. Silva-Rodrigo).

0920-5861/$ – see front matter © 2004 Elsevier B.V. All rights reserved.
doi:10.1016/j.cattod.2004.07.026

mesoporous materials, as well as their surface acidity, which in turn might promote their catalytic activity for HDT reactions [5,6].

First, the present study focused on the molecular design and synthesis of NiMo and NiW catalysts supported on Ti-MCM-41. Second, as the substitution of Si(IV) by Ti(IV) might improve the structural stability of these supports, we explored this hypothesis. The main properties of the catalysts were characterized by XRD, N_2 adsorption (BET) and NH_3-thermal programmed desorption (TPD) methods. Finally, a study of the catalytic behavior of the sulfided NiMo/Ti-MCM-41 and NiW/Ti-MCM-41 catalysts was made using thiophene as a model reaction and, on the other hand, a parallel study was made for comparison using a real feed composed of heavy vacuum gas oil (HVGO) derived from Maya crude.

2. Experimental

The MCM-41 materials were prepared following conventional methods described by Beck [7] and Schmidt [8]. The initial molar composition was 7.32NaOH:556.97-H_2O:1.65$Al(OH)_3$:H_2SO_4:6.68SiO_2:3.77CTAB [9]. The modification of the initial materials by grafting Ti^{4+} into the aluminosilicate (MCM-41) structure required sol–gel titanium oxide precursors with a molar ratio $20 < Si/Ti < 80$. For comparison, single phase TiO_2 materials were synthesized by sol gel. The bimetallic catalysts based on NiMo and NiW active phases were prepared by co-impregnation methods. Thus, the series NiMo/TiO_2-MCM-41 and NiW/TiO_2-MCM-41 catalysts were prepared by simultaneous impregnation of the support with aqueous solutions of $Ni(NO_3)_2{\cdot}6H_2O$, $(NH_4)_6Mo_7O_{24}$ and $(NH_4)_6W_{12}O_{39}{\cdot}H_2O$, respectively. In all cases, the Ni/Ni + Mo and Ni/Ni + W ratios were equal to 0.3, which is typical of the metals composition of industrial catalysts. The thermal decomposition of the original metal salts was performed by calcinations at 450 °C in air, while the catalysts activation (sulfiding) was performed ''in situ'', before carrying out the reaction [10]. For comparison, a reference NiMoP industrial catalyst was also tested. The concentration data of supports and catalysts are reported in Table 1.

Table 1
Nomenclature of supports and catalysts

Supports	Si/Ti (wt.%)	Catalysts	
		Ni-Mo	Ni-W
MCM-41	100/0	NMMCM-41	NWMCM-41
TM80	80/20	NMTM80	NWTM80
TM50	50/50	NMTM50	NWTM50
TM20	20/80	NMTM20	NWTM20
TiO_2	0/100	NMT	NWT
γ-Al_2O_3	–	NMAP[a]	NMAP[a]

[a] Reference catalyst; P: phosphorous; Ni/(Ni + Mo) = 0.3; Ni/(Ni + W) = 0.3.

The structural features of the catalysts were characterized by X-ray diffraction using a Bruker AXS diffractometer, model 8000 advance, using Cu Kα radiation and continuous sweeping of 0.6° min^{-1}, without rotation, within the interval $1.5 < 2\theta < 10$.

The textural properties of the supports were determined by N_2 adsorption (BET) at 78 K, using a Quantacrome AUTOSORB-1 sorptometer.

The surface acidity of the solids was determined by thermal programmed desorption of NH_3, using a GC-GOW-MAC 580 system fitted with a thermal conductivity detector (TCD). The samples were pretreated at 450 °C, 2 h, before ammonia adsorption at 500, 450, 400, 300 and 200 °C. The thermal desorption was scanned within the interval from 140 to 500 °C.

The hydrothermal stability of the catalysts was tested using a quartz reactor with water vapor flow (100 ml/min) at 400, 500 and 600 °C, for 2 h, at a heating rate of 2 °C/min [11].

The thiophene HDS reaction scheme is shown in Fig. 1 [20]. This reaction occurs following two main pathways: (1) direct thiophene hydrogenation leading to dihydrothiophene (DHT), then tetrahydrothiophene (THT) forms, with further C–S bonding hydrogenolysis, (2) rupture of the C–S bonding and subsequent formation of unsaturated hydrocarbons [19]. Thus, in this work HDS of thiophene was carried out at 350 °C. Before the reaction, the catalysts were pre-sulfided at 400 °C, 3 h, using a H_2/H_2S ratio of 9/1. The catalytic properties of the solids in powder form were evaluated using a batch type reactor. The initial feedstock was HVGO derived from Maya crude (2.21 wt.% S and 0.18 wt.% N_2). The reaction conditions were T = 350 °C, 12 MPa, with stirring at 250 rpm for 3 h, without diffusion limitations.

3. Results and discussion

3.1. X-ray diffraction

The X-ray diffraction patterns shown in Fig. 2 show a peak typical of mesoporous MCM-41 materials, between 2° and 3° (2θ). The hybrid Ti-MCM-41 materials TM80 showed additional XRD peaks, which have a minor intensity, arising from the hexagonal symmetry of the pore arrays. Thus, a systematic incorporation of Ti(IV)

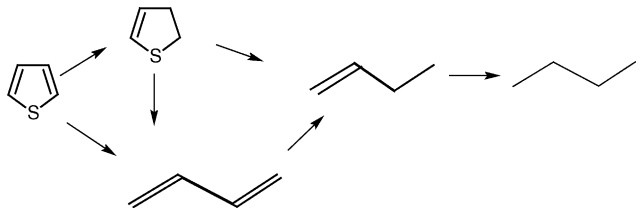

Fig. 1. Reaction pathways for thiophene HDS [20].

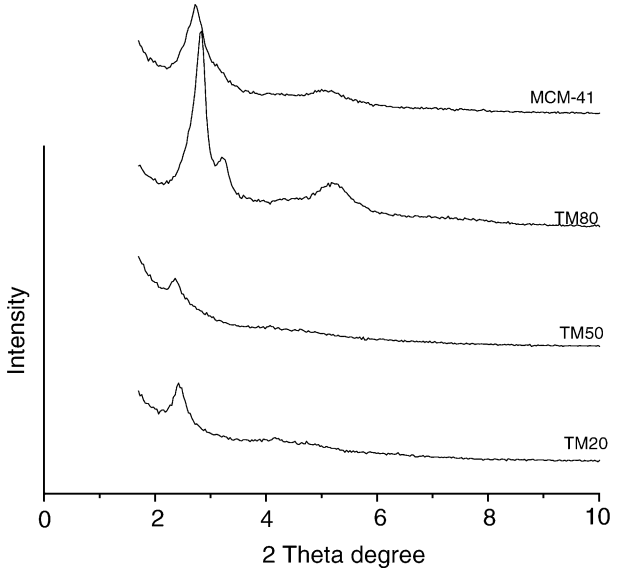

Fig. 2. XRD patterns of TiO_2-MCM-41 supports.

provokes a diminution of the XRD peak intensity (Fig. 2), as well as a loss of the typical hexagonal symmetry [12]. Also, a small peak of anatase appears at about 39° (2θ), as well as other smaller peaks at 42, 68.5, 71.5 and 81° (2θ), which are attributed to a partial solid solution of TiO_2-Al_2O_3.

3.2. Textural properties

The nitrogen adsorption isotherms of the supports and catalysts series were used to determine the surface area (S_A) and mean pore diameters (D_p). Table 2 displays the results obtained by titania grafting of the original silicate MCM-41 materials. For TM80, solids surface areas up to 1138 m^2/g were obtained, about 8% higher than original MCM-41. In contrast to this result, incorporation of the metal phases (Ni-Mo and Ni-W) provoke a drastic decrease of the surface area, down to about one-third of the original value. Also, the average pore diameter of the supports increases with Ti concentration, in the interval between 50 and 100 Å [13]. Further increase of the pore diameters for NMTM80 and NWTM50 solids might be related to the partial destruction of the pore walls upon metal loading, i.e., partial hydrolysis of the silicate–titania wall. The Type IV nitrogen adsorption–desorption isotherms (Fig. 3) indicate the presence of mesopores [14], while the H2 type hysteresis loop (IUPAC) indicate typical cylindrical channels.

Table 2
Surface area and mean pore diameters of catalysts and supports (after calcination at 540 °C)

Sample	S_A (m^2/g)	D_p (Å)
MCM-41	1004	35
TM80	1138	56
TM50	948	65
TM20	829	54
TiO_2	59	76
Catalyst NiMo		
NMMCM-41	131	64
NMTM80	359	47
NMTM50	174	47
NMTM20	164	42
NMT	50	61
Catalyst NiW		
NWMCM-41	172	52
NWTM80	25	149
NWTM50	67	140
NWTM20	50	123
NWT	30	89

3.3. Surface acidity

Table 3 shows the TPD-NH_3 results, where an increasing population of acid sites in function of TiO_2 concentration is verified. A similar effect was reported elsewhere [18] together with a systematic decrease of surface area.

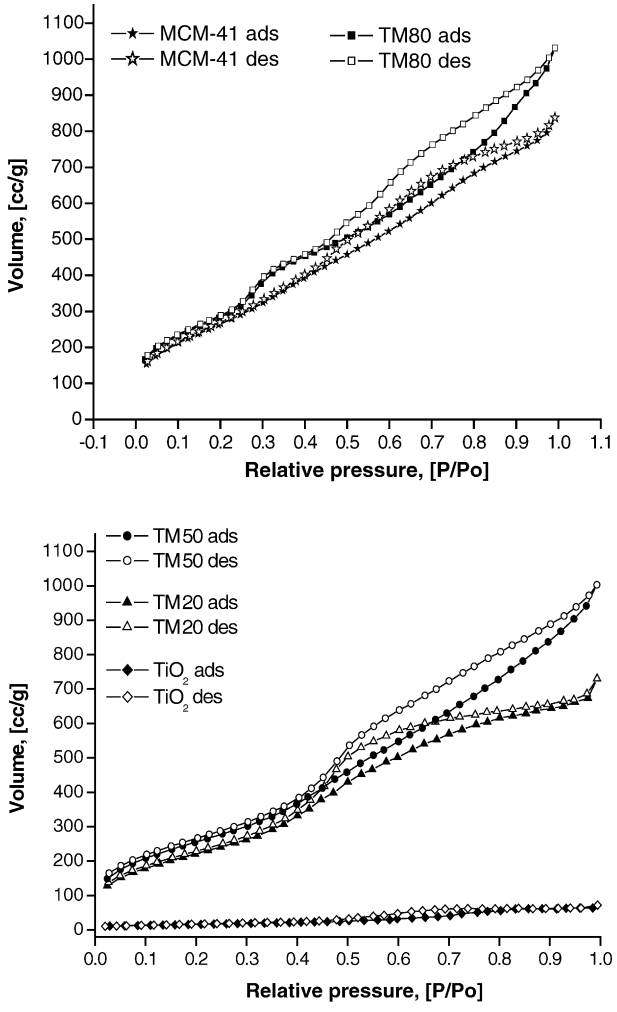

Fig. 3. N_2 adsorption–desorption isotherms at 78 K.

Table 3
Surface acidity properties of the Ti-MCM-41 supports (μmol NH_3/g)

Solids	Intrinsic acidity (μmol NH_3/g)	Specific acidity (μmol NH_3/m^2)
Supports		
MCM–41	38	0.04
TM80	53	0.05
TM50	61	0.06
TM20	62	0.07
TiO_2	114	1.93
Catalysts		
NMMCM-41	44	0.34
NMTM80	112	0.31
NMTM50	131	0.75
NMTM20	148	0.90
NMT	75	1.50
NMAP[a]		—

[a] Reference catalyst.

3.4. Hydrothermal stability

Similar to previous studies on the structural stability of MCM-41, a pore collapse was verified when the mesoporous materials were treated at about 500 °C in the presence of 100% water vapor (Fig. 4a). Afterwards, amorphous patches are left across the solids. In contrast to these results, grafting titania onto MCM-41 seems to improve the structural resistance of the original materials; as shown in Fig. 4b and c, the porous structure of TM80 and TM50 withstand up to about 600 °C and further (Fig. 4b and c) under 100% water vapor. This property might result from significant differences in hydrolysis rate of –O–Ti–O– and –O–Ti–O–Si–O bonds, with respect to –O–Si–O– bonds. Therefore, at least 20% increase of thermal resistance for the mixed series (Ti-MCM-41) was verified, which increases the potential applications of these materials under hydrotreating reaction conditions [15].

3.5. Determination of wall thickness

From the analysis of the XRD patterns and N_2 adsorption data altogether, the wall thickness (h) was determined using the methods reported elsewhere [16,17]. This parameter increases with Ti content (Table 4), while the average pore diameter remains rather close within the series TM80, TM50 and TM20 (Table 2). This trend follows the decrease of the surface area, starting with the lower Ti concentrations for the solid TM80, which presents the highest surface area, i.e., 1138 m^2/g or about 8% higher than pure MCM-41 [18], and ending with TM20, which has the lowest surface area, i.e., 829 m^2/g, but it has the highest wall thickness, i.e., 6.53 Å. Although further characterization work is necessary to explain this result, some additional porosity might be created within the original MCM-41 structure after grafting Ti ions or, alternatively, surface SiO_2-TiO_2 phases should form on the original silica walls, which should provoke a diminution

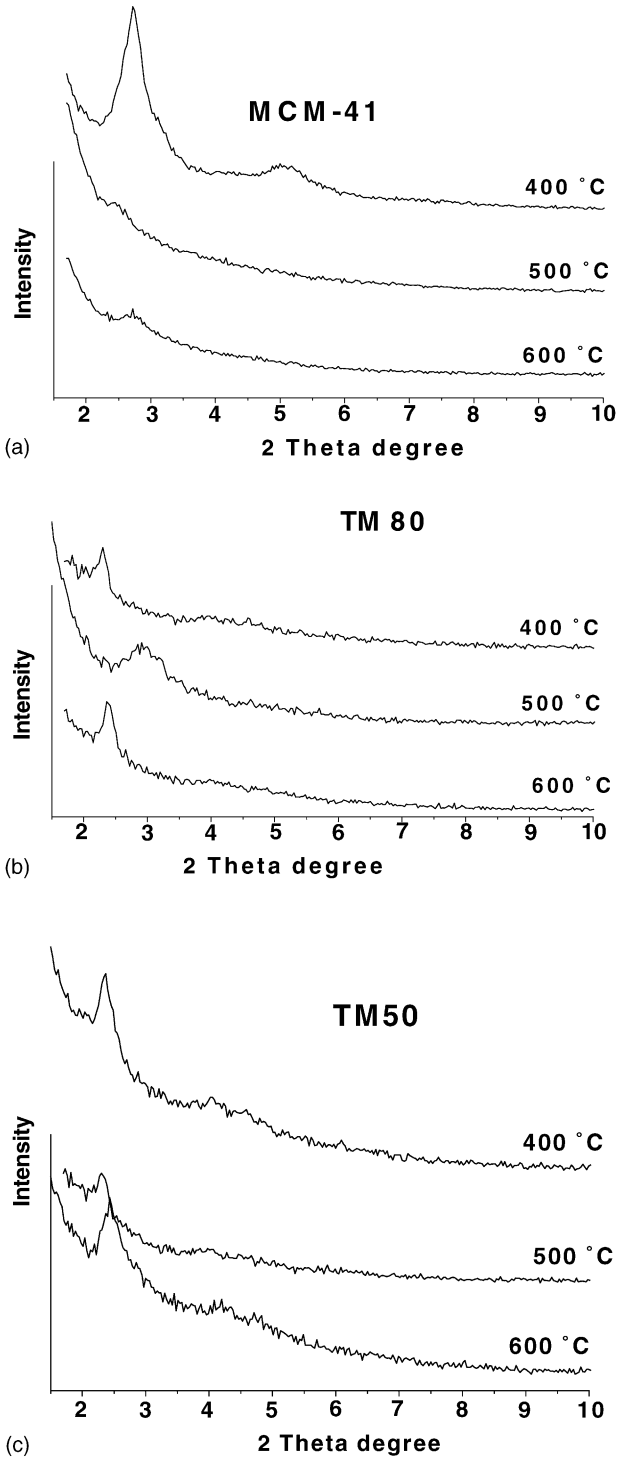

Fig. 4. XRD patterns of the calcined samples TM(X) (X = 100, 80, 50) after treatment at T = 400, 500 and 600 °C with 100% water vapor.

of the total surface area and an increase of the pore wall thickness. In any case, the surface area available is higher by a factor greater than 2 with respect to other conventional supports used in HDT, i.e., Al_2O_3. The increasing thickness of the pore walls with TiO_2 concentration indicates a surface interaction of TiO_2 with SiO_2. This is confirmed by the

Table 4
Surface area (S_A) and wall thickness (h) determined from N_2 adsorption and XRD measurements, respectively

Supports	S_A (m^2/g)	h (Å)
MCM-41	1004	5.8
TM80	1138	5.1
TM50	948	5.3
TM20	829	6.5

absence of new peaks in the XRD patterns corresponding to the pure TiO_2 phase.

3.6. Catalytic activity

The activity of the sulfided catalysts NiMo/ and NiW/MCM-41-TiO_2 are reported in Table 5. Increasing TiO_2 concentration of the supports leads to a total conversion between 9% and 24%. NMTM50 catalysts show about 18% conversion, which is lower than NMTM80 (i.e., 24% conversion), but a little higher than reference NMAP catalysts (i.e., 17% total conversion). The total conversion of tiophene on the NiMo/Ti-MCM-41 series, i.e., NMTM80, showed 30% higher activity with respect to the reference catalyst, i.e., NMAP series. This difference might be attributed to a higher metal loading on the Ti-MCM-41 materials, i.e., similar (Ni/Ni + Mo) = 0.3 with a total metal load of 2.8 atoms/nm^2. The catalysts supported on pure MCM-41 or TiO_2, i.e., NMMCM-41 and NMT, possess a catalytic activity about 10% lower than the reference catalysts (NMAP). The general trend shows a catalytic activity proportional to the metal concentration, as reported elsewhere [18]. A diminution of conversion with excess TiO_2 concentration was verified. The supported NiW catalysts showed a particular behavior, i.e., the solids having a TiO_2 concentration of 50% (NWTM50) behave similarly to NMTM80, i.e., about 24% conversion, which was about 30% superior than reference NMAP catalysts. Excepting NMTM50, the rest of the series showed a smaller conversion with respect to the reference (Fig. 5). Fig. 6 shows the selectivity of supported NiMo catalysts, which

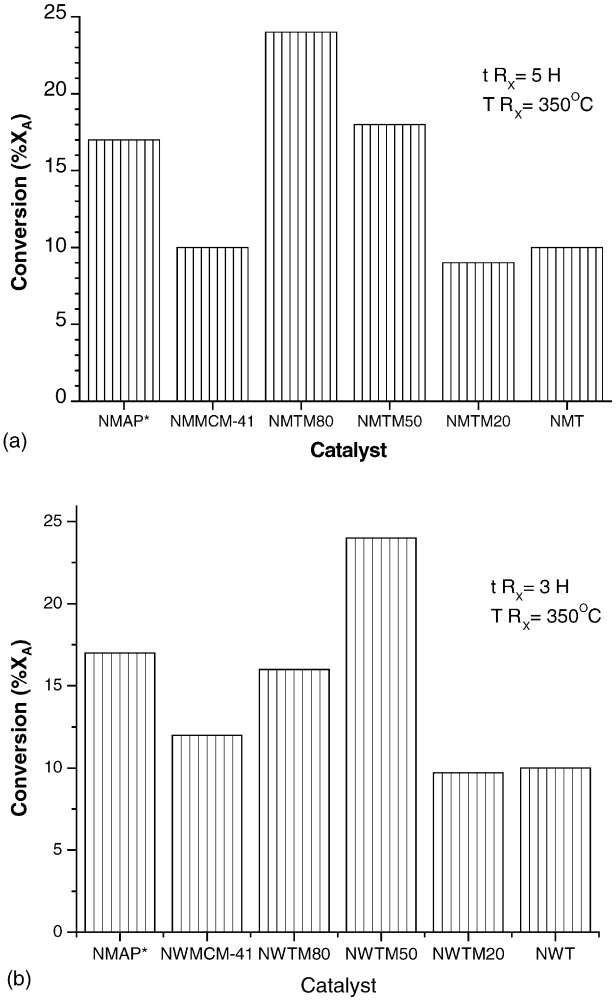

Fig. 5. Catalytic conversion of thiophene: (a) NiMo/TM(X) and (b) NiW/TM(X).

Table 5
Variation of the sulfur content after reaction on MCM-41- and Ti-MCM-41-supported NiMo, NiW catalysts, at 350 °C, P_{H_2} = 12 MPa, 3 h reaction time

Catalyst	S_{Total} (wt.%)	ΔS_{real} (%)
HVGO	4.70	–
NMMCM-41	3.22	−31.48
NMTM80	4.23	−10
NMTM50	2.94	−37.44
NMT	3.69	−21.4
NWMCM-41	3.56	−24.25
NWTM80	4.13	−12.12
NWTM50	3.01	−35.95
NWT	3.76	−20.00
NMAP*	3.89	−17.23

were more selective for n-butane formation, i.e., the average was about 58%, the rest being orientated towards olefins and cracking products (C_1–C_3). From Fig. 6, the selectivity of the NMTM(X) catalysts series showed up slightly higher with respect to the reference catalysts, but a higher proportion of olefins was obtained with respect to the reference catalysts.

Table 5 shows the HDS results of real feedstock, i.e., HVGO derived from Maya crude, at 350 °C, P_{H_2} =12 MPa. The highest sulfur removal capacity corresponded to supported NMTM-50, leaving only 2.94 wt.% S in the reaction media, i.e., about 37.44 wt.% S removal, while NWTM50 showed about 35.95 wt.%. In comparison, NiMo catalysts supported on MCM-41 and TiO_2 phases showed about 31.48% and 21.4%, respectively. NWMCM-41 and NWT removed about 24.2% and 20% (S) from the real feed, respectively, against 17.23% obtained with the reference catalysts. Therefore, the behavior of the same catalysts series differ with respect to the activity profile shown by the model reaction.

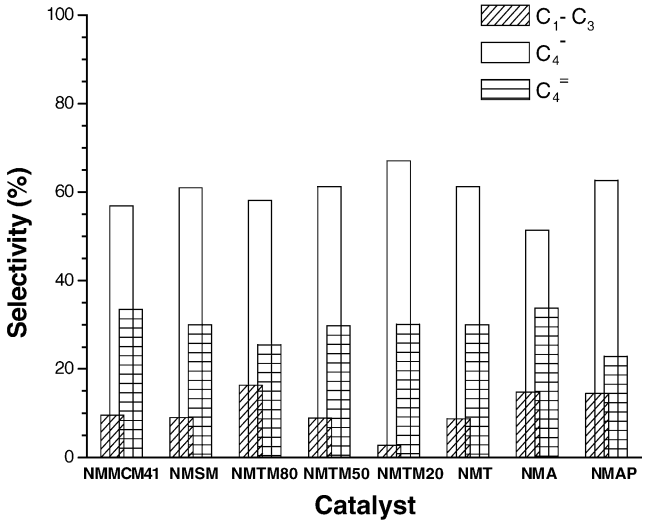

Fig. 6. Selectivity of catalysts for HDS of thiophene.

4. Discussion and conclusions

The hexagonal symmetry of the pore arrays of MCM-41 was verified by XRD. This symmetry was unchanged after grafting Ti(IV) up to about a Si/Ti ratio equal to 80/20 (wt.%). However, at a higher Ti(IV) concentration a partial loss of the pore ordering occurs, together with the appearance of small peak of TiO_2 (Anatase) at about 39° (2θ) and other smaller XRD peaks at 42, 68.5, 71.5 and 81° (2θ), belonging to a mixed phase, probably a partial solid solution of TiO_2-Al_2O_3. Also, the surface acid site density increased with Ti(IV) and metals (Ni, Mo, W) loadings, with respect to single phase MCM-41 materials. The latter effect might not be attributed to the charge unbalance associated to the Ti(IV)-substituted tetrahedral silica species ($Si^{4+}O_4^{2-}$ by $Ti^{4+}O_4^{2-}$) but to local polarizing effects arising from the differences of the bond configurations of SiO_2 and TiO_2, outer shell electrons and covalent ionic radii differences, i.e., $r_{Ti(IV)} = 1.36$ Å for the sp^3d^2 Ti(IV) octahedral bond configuration and $r_{Si(IV)} = 1.17$ Å for the sp^3 Si(IV) tetrahedral configuration. Also, there are slight differences of electronegativity (χ) between Ti and Si, i.e., $\chi_{Ti} = 1.5$ and $\chi_{Si} = 1.8$. From these properties, the ionic character was determined according to Pauling's empirical rule, i.e., $P = 46\%$ for Ti–O bond and $P = 37.3\%$ for Si–O bond. This lead us to conclude that electronic properties of the Ti-MCM-41 surface might be rather different with respect to original MCM-41 materials. In turn, these variations may induce a heterogeneous surface sites distribution that play a role for adsorption and catalysis. On the other hand, the textural properties of the catalysts, i.e., surface area (S_A), average pore diameter (D_p) and total pore volume (V_p), decreased drastically with the concentration of both Ti(IV) and metals (Ni, Mo, W). For some cases, S_A fell down to about 10% of the original MCM-41 area. Also, Type IV isotherms and H2 type hysteresis loops were common in most of these cases, which might be associated to aggregation models consisting of cylindrical channels formed by assemblies of heterogeneous sized spherical particles. In addition, grafting of Ti(IV) seemed to improve the hydrothermal resistance of the solids, from about 500 °C for single phase Si-MCM-41 (in 100% H_2O vapor) up to 600 °C for hybrid Ti-MCM-41materials. In parallel, the wall thickness (h) of the hybrid Ti-MCM-41 materials increased with Ti(IV) addition, thus enhancing further their structural stability. This additional thermal resistance may arise from the lower hydrolysis rate of –O–Ti–O– bonds with respect to –O–Si–O– bonds.

The highest catalytic activity for HDS of tiophene corresponded to NMTM80 and NWTM50, with about 24% total conversion. However, this result was not matched during HDS of HVGO, where NMTM50 and NWTM50 showed the maximal performance, with about 37.44% and 35.95% sulfur removal, respectively, followed by NMM not too far behind (i.e., about 31.4% of sulfur removal). These differences might indicate that sulfur bearing molecules contained in the real feed are rather different than model tiophene molecules; thus, distinct surface sites might be responsible for each case, in terms of surface access, surface acidity strength and acid sites distribution. One common feature is the sulfided state of the catalyst, because the presulfidation treatment before reaction. Also, the NMTM50 and NWTM50 were more suitable for conversion of complex sulfur bearing molecules, as those present in HVGO. In contrast to this situation, higher Si/Ti ratios and milder surface acidity, which are both characteristics of the NMTM80 catalysts, seemed to favor the tiophene conversion with respect to more complex molecules present in HVGO. The performance of NWTM50 catalysts was noteworthy, due to their similar catalytic activity with respect to tiophene and more complex sulfur bearing molecules (HVGO) conversion. The promotional effect of Ti(IV) enhances the tiophene conversion, but it is less important in the real feed, i.e., NiMo/MCM-41 causes 31.4% sulfur removal from HVGO. As the real feed contained more complex sulfur bearing molecules like DBT and 2,4-di-methyl-DBT, the HDS reactions occur differently with respect to simple tiophene. However, the high conversion shown by NMTM50 and NWTM50 catalysts does not correlate neither with mesoporosity nor enhanced surface acidity, but a combination of surface sites and their distribution seems to play a role for enhancing the HDS of complex molecules, which makes the difference with respect to conventional supports like alumina.

Acknowledgments

The authors are grateful to FIES 98-67III from IMP and COSNET (SEP-595.02-P) for financial support.

References

[1] T. Xiao, P. York, H. Cliff, Williams, H. Wang, M.L. Green, J. Catal. 202 (2001) 100–109.
[2] M. Nagai, M. Kiyoshi, H. Tominaga, S. Omi, Chem. Lett. 6 (2000) 702–703.
[3] C. Song, C. Kwak, S.H. Moon, Catal. Today 74 (2002) 193–200.
[4] S.T. Oyama, X. Wang, F.G. Requejo, T. Sato, Y. Yoshimura, J. Catal. 209 (1) (2002) 1–5.
[5] J. Ramírez, R. Contreras, P. Castle, T. Klimova, R. Zárate, R. Moon, Appl. Catal. A: Gen. 197 (2000) 69–78.
[6] S. Parasuraman, K.B. Suresh, G.S. Chandrashekar, Ind. Eng. Chem. Head. 40 (2001) 3237–3261.
[7] J.S. Beck, US Patent 5,057,296 (1991).
[8] W. Schmidt, Stud. Surf. Sci. Catal. 84 (1994) 61–68.
[9] R. Ryoo, C. Hyun, Chem. Commun. (1999) 1413–1414.
[10] I. Bezverkhyy, P. Afanasiev, C. Geantet, M. Lacroix, J. Catal. 204 (2001) 495–497.
[11] Z. Zhang, Y. Han, F. Xiao, S. Qiu, L. Zhu, R. Wang, Y. Yu, Z. Zhang, B. Zou, Y. Wang, H. Sun, D. Zhao, Y. Wei, J. Am. Chem. Soc. 123 (2001) 5014–5021.
[12] Y. Lee, Catal. Today 38 (1997) 213–219.
[13] M. Occelli, S. Biz, A. Auroux, Appl. Catal. A: Gen. 183 (1999) 231–239.
[14] G. Leofanti, M. Padovan, G. Tozzola, Catal. Today 41 (1998) 207–219.
[15] T.R. Pauly, V. Petkov, Y. Liu, S. Billinge, T. Pinnavaia, J. Am. Chem. Soc. 124 (2002) 97–103.
[16] F. Renzo, F. Testa, J. Chen, H. Cambon, A. Galarneau, D. Plee, F. Fajula, Microporous Mesoporous Mater. (1999) 28.
[17] M.J. Meziani, J. Zajac, D. Jones, S. Partyka, J. Roziere, Langmuir 16 (5) (2000).
[18] A. Montoya, J. Meléndez-Hernández, J.M. Domínguez, G. Sandoval-Robles, Mater. Res. Soc. Symp. Proc. 431 (1996) 337;
R.F. Lobo, J.S. Beck, S.L. Suib, D.R. Corbin, M.E. David, L.E. Iton, Z.I. Zones (Eds.), Microporous Macroporous Mater. 337 (1996).
[19] M. Vrinat, M. Lacroix, M. Breysse, L. Mosoni, M. Roubin, Catal. Lett. 3 (1989) 405.
[20] J.V. Lauritsen, M. Nyberg, J.K. Nørskov, B.S. Clausen, H. Topsøe, E. Lægsgaard, F. Besenbacher, J. Catal. 224 (2004) 94–106.